Biophysical Characterization of a New Phospholipid Analogue with a Spin-Labeled Unsaturated Fatty Acyl Chain

Andreas Bunge,[†] Anne-Katrin Windeck,[‡] Thomas Pomorski,[‡] Jürgen Schiller,[†] Andreas Herrmann,[‡] Daniel Huster,[†] and Peter Müller[‡*]

[†]Institute of Medical Physics and Biophysics, University of Leipzig, Leipzig, Germany; and [‡]Humboldt University Berlin, Department of Biology, Berlin, Germany

ABSTRACT Spin-labeled analogs of phospholipids have been used widely to characterize the biophysical properties of membranes. We describe synthesis and application of a new spin-labeled phospholipid analog, SL-POPC. The advantage of this molecule is that the EPR active doxyl group is linked to an unsaturated fatty acyl chain different to saturated phospholipid analogs used so far. The need for those analogs arises from the fact that biological membranes contain unsaturated phospholipids to a large extent. The biophysical properties of SL-POPC in membranes were characterized using EPR and NMR spectroscopy and compared with those of the saturated spin-labeled phospholipid, SL-PSPC. To this end, POPC membranes were labeled with either analog to assess whether the spin-labeled counterpart SL-POPC mimics the membrane properties better than the often used SL-PSPC. The results show that SL-POPC and SL-PSPC explore different molecular environments of the bilayer, and that the type and degree of perturbation of bilayer caused by the label moiety also differs between both analogs. We found that SL-POPC is more appropriate to assess the versatile dynamics of POPC membranes than SL-PSPC.

INTRODUCTION

Phospholipids are the main component forming the bilayer structure of biological membranes. Due to their amphiphilic properties they determine the physico-chemical parameters of membranes. However, phospholipids not only determine the structure of membranes, they are also specifically involved in physiological membrane-associated processes, which comprise e.g., signal transduction events, protein sorting, and the regulation of protein activity. Consequently, for decades there has been an enormous interest in the characterization of lipid structure and dynamics in model and biological membranes, using a large spectrum of biochemical and biophysical methods and assays. To cover all modes of lipid motion, techniques that do not rely on probes, such as infrared (1) and NMR spectroscopy (2–4) as well as x-ray diffraction (5) were complemented by fluorescence and EPR methods to assess motions with characteristic correlation times on the order of 10^{-7} to 10^{-10} s. However, natural phospholipids lack properties that make them amenable to EPR or fluorescence spectroscopy. Therefore, labeling techniques have been developed to (bio)-chemically introduce fluorescence or EPR active groups into phospholipids. As a result, a variety of phospholipid analogs has been synthesized and used in numerous studies. Analogs differ with respect to the label moiety used, the labeling site of the phospholipid (i.e., headgroup, *sn-1* or *sn-2* fatty acyl chain, chain position), the phospholipid species (with regard to headgroup, fatty acyl composition and type of linkage between glycerol backbone and fatty acyl residues). By using those analogs, the structural and dynamical properties of phospholipids in model and biological membranes have been characterized that are i), lateral and transverse lipid mobility in a membrane leaflet (6,7), ii), transbilayer lipid movement and distribution (8), iii), lipid-protein/peptide interaction (9–12), iv), membrane-protein interaction (9,11), v), intracellular lipid trafficking (13,14), vi), lipid metabolism and catabolism (13,15,16), vii), membrane fusion (17,18), viii), domain formation (19,20), ix), membrane protein topology (21–23), and many other membrane related phenomena. In studies using phospholipid analogs a putative influence of the probe on the process investigated has to be considered (24).

EPR spectroscopy using spin-labeled analogs has the special advantage that EPR spectra are sensitive to motions in the nanosecond timescale, which is a characteristic correlation time of phospholipid motion in biological membranes. Therefore, spin-labeled phospholipids have been applied mainly for characterizing the dynamics of phospholipids in membranes using various headgroup or fatty acyl chain-labeled analogs (25). For the latter, analogs have been used bearing the label moiety at different positions of the fatty acyl chain offering the possibility to investigate physical properties at different depth of the hydrophobic membrane core (26). The collection of available spin-labeled phospholipids is limited by the intricacy of chemical synthesis. For

Submitted May 30, 2008, and accepted for publication October 21, 2008.

*Correspondence: peter.mueller.3@rz.hu-berlin.de

Andreas Bunge and Anne-Katrin Windeck contributed equally to this work.

Abbreviations used: HBS: HEPES buffered saline; LUV, large unilamellar vesicle(s); MAS, magic-angle spinning; MLV, multilamellar vesicle(s); PC, phosphatidylcholine; POPC, 1-palmitoyl-2-oleoyl-*sn*-glycero-phosphocholine; SL-POPC, 1-palmitoyl-2-oleoyl-(16-doxyl)-*sn*-glycero-phosphocholine; SL-PSPC, 1-palmitoyl-2-stearoyl-(16-doxyl)-*sn*-glycero-phosphocholine; SUV, small unilamellar vesicle(s).

Editor: Edward H. Egelman.

0006-3495/09/02/1008/8 $2.00

doi: 10.1016/j.bpj.2008.10.037

example, typically all spin-labeled phospholipid analogs used so far contain fully saturated fatty acyl residues. However, in biological membranes a significant portion of the phospholipids features unsaturated fatty acyl chains, which are linked mainly to the *sn-2* position. Unsaturated fatty acyl residues play a decisive role in the general structure and dynamics of the membrane and in protein-lipid interaction (27–29). In this study, we use a newly synthesized spin-labeled analog of an ubiquitously occurring unsaturated phosphatidylcholine, SL-POPC structure (Fig. 1). The biophysical properties of this analog in POPC model membranes are characterized by using EPR and NMR spectroscopy and compared with those of the respective saturated analog SL-PSPC with the aim to examine which of the two analogs reflects better membrane properties.

MATERIALS AND METHODS

Chemicals

POPC and SL-PSPC were purchased from Avanti Polar Lipids (Alabaster, AL) and used without further purification. All other chemicals were from Sigma-Aldrich Chemie GmbH (Taufkirchen, Germany). HBS contained 150 mM NaCl, 5 mM HEPES (pH 7.4).

Synthesis of SL-POPC

The structure of SL-POPC is shown in Fig. 1. Its synthesis is described in detail in the Supporting Material. Briefly, our synthetic design involved two building blocks: a), 7-doxyl-nonanal **3** made in six steps from monoethylpimelate; and b), 8-carboxyl octyltriphenylphosphonium bromide **5**. 16-Doxyl oleic acid **6** was then formed from **3** and **5** by Wittig reaction followed by the coupling step to LysoPC (see Supporting Material).

Vesicle preparation

For NMR measurements, mixtures of phospholipids and sterols were prepared in a chloroform-methanol mixture (1:1 v/v). The solvent was removed by rotary evaporation and the resulting lipid film was redissolved in cyclohexane and lyophilized overnight to obtain a fluffy powder. Samples were hydrated with 40 wt % water and equilibrated by 10 freeze-thaw cycles and gentle centrifugation. The resulting multilamellar lipid dispersions were transferred into 5-mm glass vials for static ^{2}H NMR experiments. For ^{1}H MAS NMR experiments, samples were filled into 4-mm high-resolution MAS rotors with spherical Kel-F inserts. For ^{13}C NMR experiments samples were transferred to 4-mm MAS rotors with cylindrical sample volume and a Teflon insert. The samples were stored in a −70°C freezer before NMR experiments.

For EPR measurements, aliquots of lipids (labeled and nonlabeled) in organic solution were transferred to a glass tube and dried under nitrogen. The lipids were resuspended in a small volume of ethanol and HBS was added to give a final lipid concentration of 5 mM (final ethanol concentration was <1% (v/v)) resulting in the formation of MLV. To prepare LUV, five freeze-thaw cycles were carried out followed by extrusion of the MLV solution 10 times at 40°C through two 0.1-μm polycarbonate filters (mini-extruder from Avanti Polar Lipids; filters from Costar, Nucleopore GmbH, Tübingen, Germany).

EPR measurements

Samples for the EPR measurements were transferred to 50 μl micropipettes (Brand, Wertheim, Germany), sealed by modeling material and filled into quartz capillaries (4 mm internal diameter, Bruker, Karlsruhe, Germany). EPR spectra were recorded at an EMX spectrometer (Bruker). For recording EPR spectra of analogs, the following parameters were used: modulation amplitude, 1 G; power, 20 mW; scan width, 100 G, accumulation, 9 times. To quantify the mobility of labeled lipid a correlation time of rotation was calculated from the spectra (30,31).

Ascorbate assay

POPC-LUV (5 mM) were symmetrically labeled with the phospholipid analogs (2 mol %). At time zero of the kinetics, LUV were mixed with ascorbic acid in HBS (from a stock solution adjusted to pH 7.4; final ascorbate concentration 20 mM). EPR spectra were recorded at 30°C at different times using a Bruker EMX spectrometer (parameters: modulation amplitude, 2 G; power, 20 mW; scan width, 50 G, without accumulation). The decrease of the EPR signal intensity was estimated by relating the height of the low field peak of EPR spectra to those in the absence of ascorbic acid.

NMR measurements

Solid state ^{2}H NMR spectra were recorded on a wide bore Bruker Avance 750 NMR spectrometer (Bruker BioSpin, Rheinstetten, Germany) at a resonance frequency of 115.1 MHz (magnetic field strength of 17.6 T) using a single channel solid probe with a 5 mm solenoid coil. The ^{2}H NMR spectra were accumulated using the quadrupolar echo sequence and a relaxation delay of 2 s (32). The two 2.5-μs $\pi/2$ pulses were separated by a 60 μs delay. Typically, 512 scans with a spectral width of 500 kHz were acquired. For all experiments, the carrier frequency of the spectrometer was placed in the center of the spectrum. The free induction decays were left-shifted after acquisition to initiate Fourier transformation on top of the quadrupolar echo. Only data from the real channel were processed to yield symmetrized ^{2}H spectra with a better signal/noise ratio.

^{2}H NMR spectra were dePaked (33) and smoothed order parameters (34) for each methylene group in the chain were determined from the observed quadrupolar splitting $\Delta\nu_Q^{(i)}$ for the i_{th} chain segment according to

$$\left|\Delta\nu_{\text{Q}}^{(\text{i})}\right| = \frac{3}{4}\chi_Q\left|S_{\text{CD}}^{(\text{i})}\right|. \quad (1)$$

Here, $\chi_Q = e^2qQ/h$ represents the quadrupolar coupling constant (167 kHz for the C–^{2}H bond), $S_{\text{CD}}^{\text{i}} = 1/2\langle 3\cos^2\theta_{\text{i}} - 1\rangle$ is the segmental order parameter, θ is the angle between the bilayer director and the external magnetic field B_0.

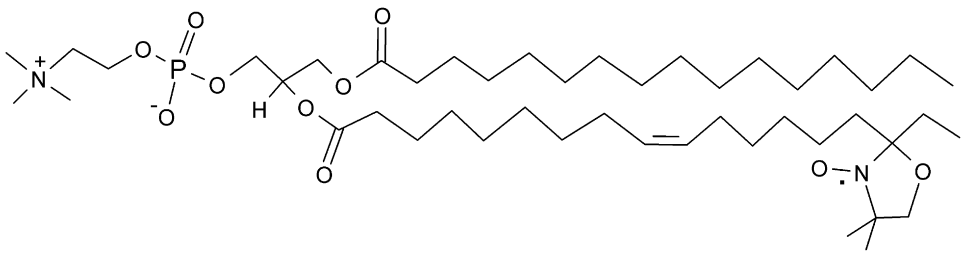

FIGURE 1 Structure of SL-POPC.

The Pake doublets were assigned starting from the terminal methyl group exhibiting the smallest quadrupolar splitting. The methylene groups were assigned successively according to their increasing quadrupolar splittings. The smoothed order parameter profiles were determined from the observed quadrupolar splittings as described in detail by Huster et al. (35). Average order parameters were calculated by adding all chain order parameters and dividing them by the number of methylene and methyl groups in the chain.

The chain extension L_C^* can be estimated by projection of the averaged length of the carbon segments on the bilayer normal and summation over successional carbon segments. The first moment of the deuterium spectra was calculated according to:

$$M_1 = \int_0^\infty \omega f(\omega) d\omega \Big/ \int_0^\infty f(\omega) d\omega, \qquad (2)$$

where $f(\omega)$ is the spectral intensity distribution and $\omega = 0$ corresponds to the Larmor frequency ω_0.

^{1}H and ^{13}C MAS NMR spectra were acquired at a spinning speed of 8 kHz on a Bruker Avance 750 NMR spectrometer operating at 749.69 MHz for ^{1}H NMR and 188.53 MHz for ^{13}C, respectively, using a double resonance CP MAS probe equipped with a 4-mm spinning module. Typical $\pi/2$ pulse lengths were 5 μs. ^{1}H T_1 relaxation times were measured using the inversion recovery pulse sequence with 16 time delays between 1 ms and 4 s, a relaxation delay of 4 s, and a spectrum width of 8 kHz. ^{13}C single pulse excitation spectra were accumulated at a spinning frequency of 8 kHz, a spectrum width of 50 kHz, and TPPM decoupling at a ^{1}H decoupling field of ~50 kHz. Typical $\pi/2$ ^{13}C excitation pulse lengths were 5 μs. ^{13}C T_1 relaxation times were measured using the inversion recovery pulse sequence with 13 delays between 1 ms and 6–12 s and a relaxation delay of 12 s.

The observed relaxation rates $R_1 = 1/T_1$ for each lipid segment in the presence of the unpaired electron in the spin label are the sum of paramagnetic and dipolar relaxation rates ($R_1 = R_{1,p} + R_{1,d}$) (22). $R_{1,p}$ can be easily determined by subtracting $R_{1,d}$ measured in the absence of the spin label. All spectra were acquired at a temperature of 30°C.

RESULTS

EPR spectra of SL-POPC incorporated into membranes

POPC lipid vesicles were labeled with either SL-POPC or SL-PSPC and the recorded EPR spectra were compared (Fig. 2). As typical for spin-labeled lipids, spectra reflect a restricted mobility of the label moiety (26). A comparison of the spectra of SL-POPC and SL-PSPC recorded at 4°C indicates a somewhat higher mobility for SL-PSPC as seen from the narrower peaks of this analog (see low field and mid field peaks in Fig. 2 *E*). Likewise, the spectra recorded at 30°C reflect similar differences in the analog mobility, however, the differences between the spectra were rather low. To quantify those differences, we have recorded the EPR spectra of SL-POPC and SL-PSPC at different temperatures and calculated the correlation time of rotation (τ) from the spectra (Fig. 3). As expected, τ decreased with increasing temperatures reflecting alterations in the mobility of the probe. In agreement with the qualitative differences of the EPR spectra (Fig. 2), the correlation time of rotation is slightly lower for SL-PSPC compared to SL-POPC at 4°C. This difference in correlation times between both analogs becomes smaller at higher temperatures vanishing at $\geq$20°C, i.e., both analogs show a similar mobility at those temperatures (see Discussion).

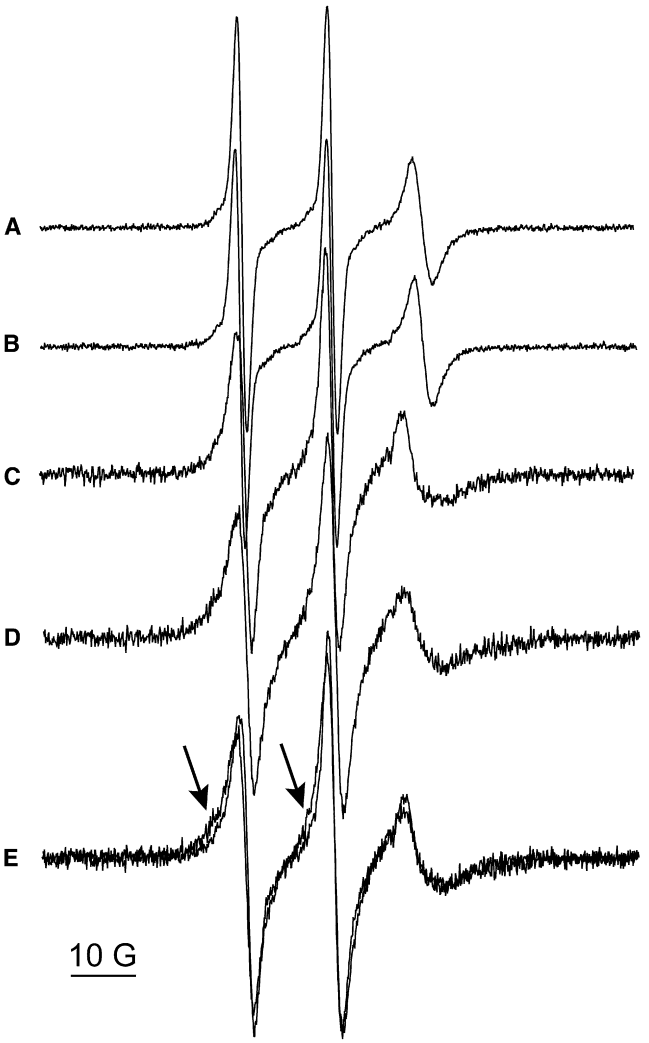

FIGURE 2 EPR spectra of spin-labeled PC analogs in POPC membranes. Multilamellar vesicles consisting of 5 mM POPC and 0.5 mol % SL-PSPC (*A* and *C*) or SL-POPC (*B* and *D*) were prepared and spectra were recorded at 30°C (*A* and *B*) and at 4°C (*C* and *D*). (*E*) Spectra for both analogs recorded at 4°C (*C* and *D*) are superimposed to visualize differences between both spectra that are indicated by the arrows. The narrower and broader peaks belong to the spectrum of SL-PSPC and SL-POPC, respectively.

To characterize the lateral dynamics of the analogs in the membrane, EPR spectra were recorded from lipid vesicles containing varying fractions of SL-POPC or SL-PSPC, respectively. It is known that an increase of label concentration resulting in shorter distances between analog molecules may cause an increased spin-spin interaction, which can be followed from a broadening of EPR signals (36). Indeed, as illustrated in Fig. 4 for the midfield peak (H_0) we observed an increase of the line width with increasing analog concentration for both analogs at 4°C and 30°C. Comparing the data of SL-POPC and SL-PSPC, the line widths are similar for both analogs at 30°C with the exception at 20 mol %.

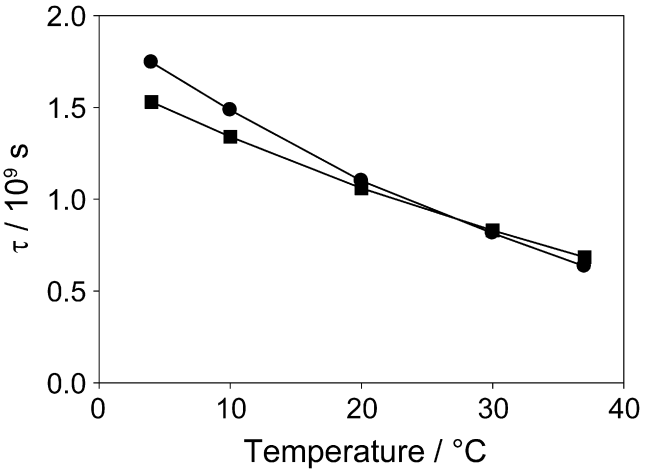

FIGURE 3 Influence of temperature on the rotational correlation time (τ) of the doxyl moiety in spin-labeled PC analogs. Multilamellar vesicles consisting of 5 mM POPC and 2 mol % SL-PSPC (■) or SL-POPC (●) were produced and spectra were recorded at different temperatures. Data represent the mean of two independent measurements.

However, at 4°C SL-POPC and SL-PSPC behave differently. Although the line width of SL-PSPC only slightly increases with analog concentration, it shows a distinct increase for SL-POPC.

Characterization of the membrane localization of the doxyl moiety of SL-POPC by EPR

To characterize the localization of the label moiety within the hydrophobic membrane core we measured the accessibility of the doxyl group for the soluble EPR signal quencher ascorbic acid. Ascorbic acid reduces the spin label resulting in a loss of signal intensity of the corresponding EPR spectra (37). Recording the EPR data of SL-PSPC or SL-POPC in POPC-LUV on addition of ascorbic acid, we observed a decrease in signal intensity for both analogs, which was faster for SL-POPC (Fig. 5). To quantify these differences, the reduction kinetics were fitted to a single-exponential, yielding rate constants of $6.5 \times 10^{-4}\ s^{-1}$ and $4.3 \times 10^{-4}\ s^{-1}$ for SL-POPC and SL-PSPC, respectively. To estimate the insertion depth of the label moiety based on reduction kinetics, we measured the ascorbate-mediated loss of signal intensity for the spin-labeled phosphatidylcholine analog 1-palmitoyl-2-(4-doxylpentanoyl)-*sn*-glycero-3-phosphocholine. The label moiety, which is attached to the short chain fatty acyl residue in *sn-2* position is very close to the membrane surface. Indeed, the decline of the EPR signal on addition of ascorbate was very rapid (Fig. 5). This suggests that the label moiety of SL-POPC is more deeply inserted into the hydrophobic region of the membrane and even more that of SL-PSPC.

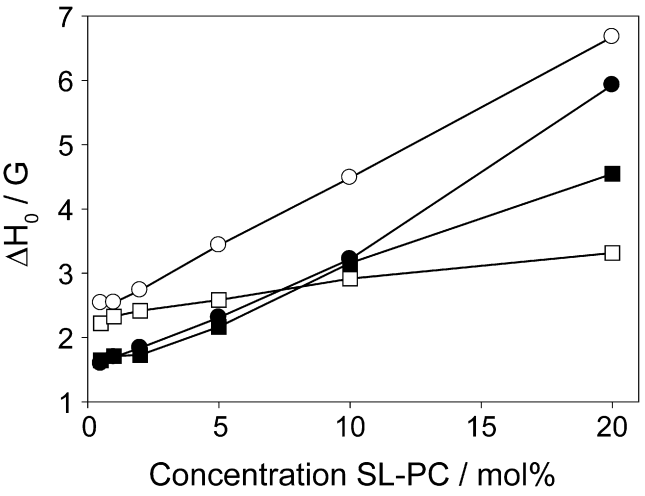

FIGURE 4 Influence of the analog concentration on the line width of EPR spectra. Multilamellar vesicles consisting of POPC and different concentrations of SL-PSPC (*squares*) or SL-POPC (*circles*) were produced (giving a final lipid concentration of 5 mM) and spectra were recorded at 4°C (□, ○) or at 30°C (■, ●). From the spectra the line width of the midfield peak ΔH_0 was extracted.

Influence of SL-POPC on membrane structure

To study the influence of the spin label moiety on the chain packing properties in the host membrane, ^2H NMR experiments were carried out. The quadrupolar splittings of the ^2H NMR spectra of POPC-d_{31} membranes in the presence of SL-POPC at a molar ratio of SL-POPC/POPC-d_{31} (mol/mol) 1:20, 1:10, and 1:4 are slightly reduced (data not shown). From these spectra smoothed order parameter profiles and difference order parameter profiles were extracted (Fig. 6). At low concentration (molar ratio of

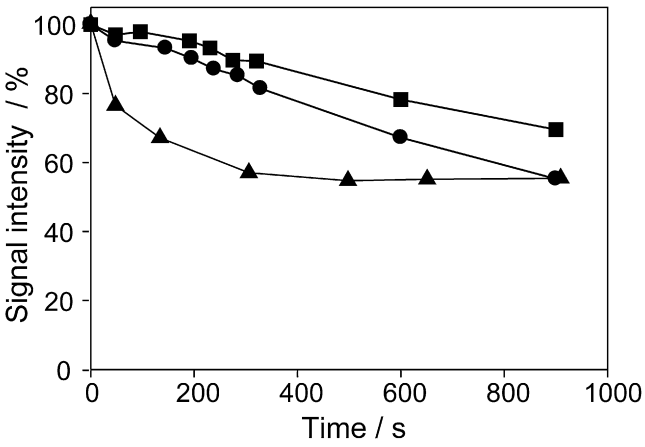

FIGURE 5 Kinetics of ascorbate-mediated EPR signal reduction of spin-labeled PC analogs in POPC vesicles. Large unilamellar vesicles consisting of 5 mM POPC were symmetrically labeled with 2 mol % SL-PSPC (■), SL-POPC (●) or 1-palmitoyl-2-(4-doxylpentanoyl)-*sn*-glycero-3-phosphocholine (▲) as described in Materials and Methods. At time point zero, labeled LUV were mixed with ascorbic acid (to give a final concentration of 20 mM) and transferred to an EPR capillary. Subsequently, EPR spectra were recorded at the given time points at 30°C. From the spectra the signal intensity of the low field peak was estimated and normalized to that in the absence of ascorbate.

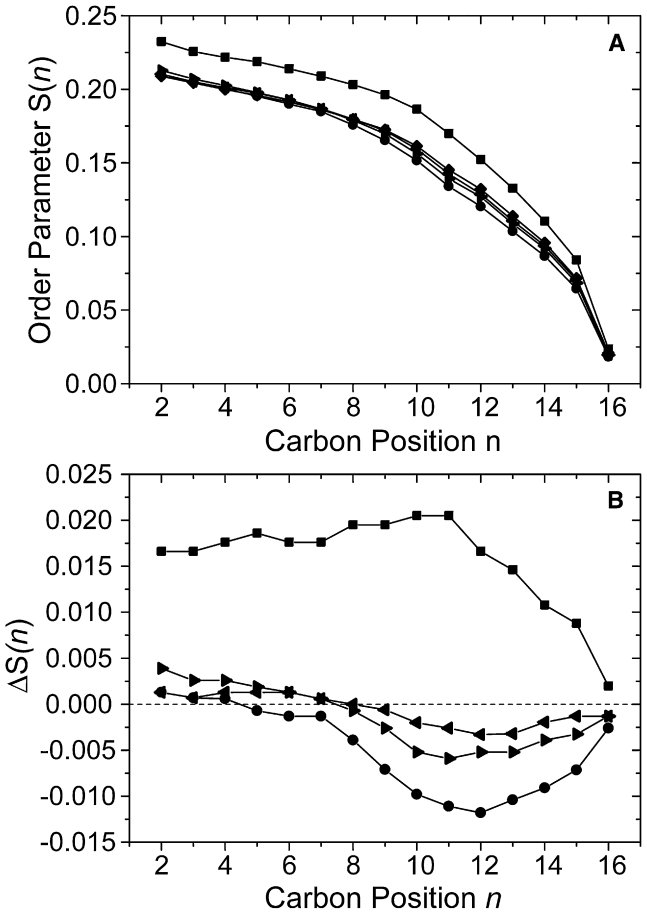

FIGURE 6 Smoothed ^{2}H NMR order parameter profiles for pure POPC-d_{31} membranes (◆) in the presence of SL-POPC at a molar ratio of SL-POPC/POPC-d_{31} (mol/mol) 1:20 (◀), 1:10 (▶), and 1:4 (●) and in the presence of SL-PSPC at a molar ratio of SL-PSPC/POPC-d_{31} (mol/mol) 1:4 (■) (*A*). (*B*) Difference order parameter profiles of POPC-d_{31} in the binary mixtures with respect to pure POPC-d_{31} membranes. In the presence of SL-POPC the order parameters of POPC-d_{31} are reduced slightly, especially in the lower chain region. SL-PSPC increases the order of the upper/middle part of the hydrocarbon chains of the POPC-d_{31} membrane. The order parameter profile for SL-PSPC was adapted from Vogel et al. (22) for comparison.

SL-POPC/POPC-d_{31} (mol/mol) 1:20), SL-POPC has only a minor influence on the order parameter of the *sn-1* chain of POPC-d_{31}. However, at higher label concentrations the order parameter is decreased in the lower and middle region of fatty acyl chains compared to that in the absence of the analog. These data are compared with the results of a study characterizing the impact of SL-PSPC on lipid packing in membranes using the same approach (22). SL-PSPC causes order parameter changes of the *sn-1* chain of POPC-d_{31}, which are more pronounced than those of SL-POPC (Fig. 6 *B*, only shown for SL-PSPC with a molar ratio of SL-PSPC/POPC-d_{31} (mol/mol) 1:4). In contrast to SL-POPC, the changes of the order parameter in the presence of SL-PSPC mainly concern the upper and middle part of the hydrocarbon chains of the host membrane.

Characterization of the membrane localization of the doxyl moiety of SL-POPC and SL-PSPC

Given the fact that the paramagnetic doxyl groups enhance the relaxation rates of nuclear spins by a paramagnetic contribution, the distribution of the chain-attached doxyl groups in the membrane can be studied. By plotting the ^{1}H paramagnetic relaxation rate for each lipid segment as a function of the corresponding coordinates with respect to the bilayer normal, further differences between the SL-POPC and SL-PSPC are obvious both at low and high temperature (Fig. 7). At 30°C the spin label moieties of both analogs are

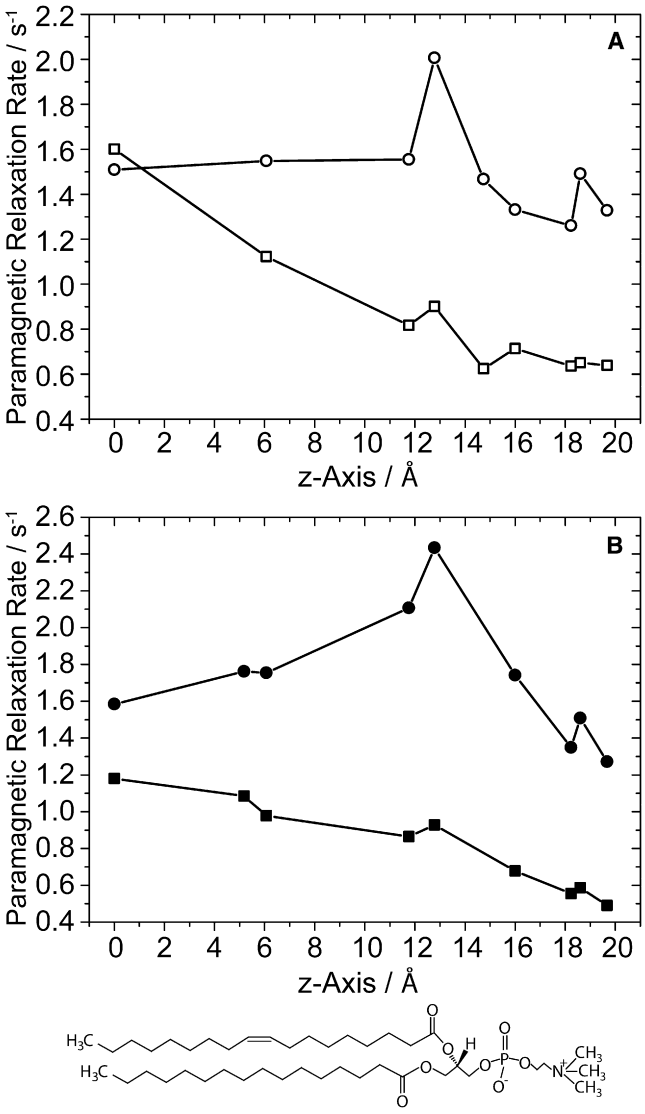

FIGURE 7 ^{1}H paramagnetic relaxation rates of POPC lipid segments in the presence of SL-POPC (*circles*) or SL-PSPC (*squares*) as a function of the coordinates of such lipid segments (Scott Feller, Wabash College, Crawfordsville, IN, personal communication, 2006) at 4°C (*A*) (□, ○) and 30°C (*B*) (■, ●) at a molar ratio of POPC/spin-labeled lipid of 200:1 and a water content of 40 wt %. The paramagnetic relaxation rates for SL-PSPC at 30°C were adapted from Vogel et al. (22) for comparison.

broadly distributed in the bilayer membrane (Fig. 7 *B*). The probability of the location of the doxyl label of SL-POPC in POPC membranes has a maximum in the upper chain/glycerol region and decreases toward the headgroup and lower chain region. In contrast, for SL-PSPC the ^{1}H paramagnetic relaxation rates increase gradually from the headgroup to the center of the bilayer. At 4°C the label moiety of SL-POPC also remains widely distributed with respect to the bilayer normal with a preference for the upper chain region (Fig. 7 *A*). For SL-PSPC the probability distribution shows a stronger increase toward the bilayer center at 4°C compared to 30°C indicating less frequent contacts of the doxyl group with the upper chain region of POPC.

Similar conclusions can be drawn from the analysis of the ^{13}C paramagnetic relaxation rates (Fig. 8). At 30°C the probability of distribution of the spin label for SL-POPC is highest in the upper chain/glycerol region whereas for SL-PSPC the highest ^{13}C paramagnetic relaxation rates can be found close to the CH_3 groups at the lower chain region of the POPC membrane.

DISCUSSION

In the current study we characterize the biophysical properties of a newly synthesized spin-labeled phosphatidylcholine analog, SL-POPC, with an unsaturated oleoyl residue on the *sn-2* position, which also bears the spin label moiety. To the best of our knowledge solely saturated spin-labeled phospholipid analogs have been applied in biophysical membrane studies. However, biological membranes consist to a large extent of unsaturated phospholipids. Therefore, by complementing spin-labeled saturated phospholipids, this analog will allow to mimic physiological relevant lipids and their molecular environment much better. Here, the properties of SL-POPC were compared with those of the respective saturated analog SL-PSPC using various EPR and NMR experiments. Despite the fact that SL-PSPC has often been used to study membranes, endogenous PSPC is, in contrast to POPC, a phospholipid occurring very rarely.

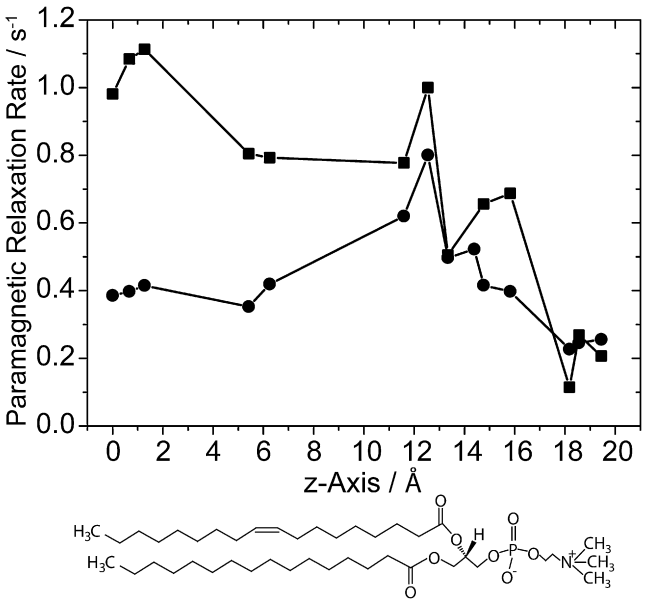

FIGURE 8 ^{13}C paramagnetic relaxation rates of lipid segments of POPC in multilamellar vesicles as a function of the lipid coordinates of such lipid segments at 30°C in the presence of 2 mol % SL-POPC (●) or SL-PSPC (■) and a water content of 40 wt %. The ^{13}C paramagnetic relaxation rates for SL-PSPC at 30°C were adapted from Vogel et al. (22).

By measuring paramagnetic relaxation rates, we explored the localization and distribution of the spin label moiety along the membrane normal. Typically, chain attached probes are broadly distributed (38,39). The probability for the localization of the doxyl probe of SL-PSPC decreases from the bilayer center to the headgroup showing that the label group is localized with largest probability around the position inferred from a rigid all-*trans* configuration of the acyl chain (22). The finite probability observed for the localization of the spin probe in the headgroup region, which is caused most likely by upturning chains indicates high dynamics of the fatty acyl chains (40).

The distribution function of the spin moiety of SL-POPC differs from that of SL-PSPC. Most significantly, in contrast to SL-PSPC the paramagnetic relaxation rates indicate a preferred localization of the doxyl group of SL-POPC in the upper chain and glycerol region. One may wonder whether such a localization could be explained by a back folding of the labeled fatty acyl chain as it has been found for the chain-attached fluorescence probe NBD of respective phospholipid analogs (38,39). The fixed charge of the NBD group interacts most favorably with the polar environment of the lipid/water interface of the membrane thereby forcing the fatty acyl chain to back-fold.

However, as judged from phospholipids with doxyl-labeled saturated fatty acyl chains such as SL-PSPC, the comparatively apolar nature of the doxyl moiety is not able to drive back folding of fatty acyl residues. This is underlined by the experimental finding that the localization probability of the doxyl group is highest in the hydrophobic core of the membrane, i.e., at the bilayer center, where it experiences attractive van der Waals interactions. Hence, the preferred localization of the doxyl label of SL-POPC reflects a property of unsaturated fatty acyl chains, but not a property of the spin label.

^{2}H NMR order parameters were studied to investigate the influence of the label group on lipid chain packing properties. Analysis of the membrane order parameter shows an increase in chain order in the upper/middle chain region of the membrane in the presence of SL-PSPC (22). This behavior is in agreement with the broad distribution of the spin probe along the whole acyl chain region resulting in an increase of packing density. The bulky doxyl group occupies a volume of 142 $Å^3$, which compares with the volume of approximately five CH_2 groups. Thus, the free volume in the membrane is reduced by insertion of the doxyl

probe, which decreases the motional freedom of the acyl chains and, therefore, increases chain order parameters.

In contrast, in the presence of SL-POPC we observed only relative small alterations of membrane packing even in the presence of very high concentrations of SL-POPC. The order parameters are only slightly reduced mainly in the lower chain region. This leads to the conclusion that SL-POPC reflects the properties of natural membranes much better in particular the incredible motional freedom of the lipid chains.

A different localization of the doxyl group of both analogs can be also inferred from the reduction kinetics of the spin label on addition of ascorbate. The loss of signal intensity was faster for SL-POPC than for SL-PSPC. This implies that in case of SL-POPC the spin label is located more closely to the lipid/water interface being more accessible to the water soluble ascorbate. As discussed above, we can rule out that the differences in reduction could be explained by a larger perturbation of the membrane structure in the presence of SL-POPC compared with SL-PSPC allowing an easier penetration of ascorbate into the membrane at these conditions: i), the analog concentration was comparatively low for the reduction experiments (2 mol %) and the NMR order parameter measurements showed a very small influence of those low analog concentrations on fatty acyl chain order; and ii), in contrast to SL-PSPC, perturbation of bilayer structure by SL-POPC was marginal.

The differences in localization of the doxyl moiety may also account for the slightly slower motions of SL-POPC below 10°C as indicated by the enhanced rotational correlation time τ of the analog with respect to SL-PSPC. We assume that the larger probability of the SL-POPC doxyl group to be localized in the upper and middle chain region as observed in the NMR measurements, is reflected in a decreased probe mobility. There is a well known gradient of motional freedom along the fatty acyl chains with the region near the headgroups being more immobilized and the mobility increasing toward the terminal methyl groups (3,26). Indeed, in case of a permanent localization of the label group in the upper membrane region one would record a much more immobilized spectrum as seen from the membrane spectrum of the analog 1-palmitoyl-2-stearoyl-(5-doxyl)-*sn*-glycero-3-phosphocholine that bears the doxyl group on the 5th carbon of the fatty acyl chain (25). At higher temperatures (above 20°C), the rotational correlation time was similar for SL-POPC and SL-PSPC indicating that the fast motions of both chains are very similar. However, this does not represent a contradiction to the NMR results. First, averaged position of the probes in the membrane is not influenced by the correlation time of their motion. Second, EPR and NMR are typically sensitive to different timescales, where NMR typically probes somewhat slower motions.

Finally, the different behavior of the line width of the midfield peak ΔH_0 with increasing label concentration could also be explained on the basis of the observed distribution of the label moiety along the membrane normal. A preferred localization of a spin label moiety as observed for SL-POPC close to the water-lipid interface enhances the probability of spin-spin interactions and, hence increases ΔH_0, in comparison to a more smeared distribution along the membrane normal. In particular, because the upper chain region is packed more densely, the restricted reorientational and lateral mobility of the doxyl moiety in the headgroup region might be the reason for the increased dipolar broadening. Essentially, differences in line broadening between both spin-labeled lipids disappeared at higher temperature. This indicates that line broadening is due to dipole-dipole interactions of the doxyl groups, which are averaged out by enhanced mobility at higher temperature. An alternative explanation might be that clustering of SL-POPC leads to line broadening. However, we consider it very unlikely that SL-POPC has a tendency to cluster in an environment of unsaturated lipids whereas SL-PSPC does not. Furthermore, in case of a clustering line broadening would be caused by exchange (Heisenberg) interactions. This type of spin interaction is known to become predominant with increasing temperature, which was not observed.

In conclusion, although spin-labeled saturated phospholipids such as SL-PSPC have been widely used successfully to characterize physical and biological properties of membranes, the comparison between the behavior of SL-PSPC and SL-POPC and their influence on membrane properties shows significant differences. This suggests that the spin-labeled analog, which mimics the endogenous phospholipids more closely should be the preferred molecule. It is known that EPR and fluorescence probes can largely dominate the structure, dynamics and membrane organization of lipids (24,39). However, our findings suggest that the lipid chain attached doxyl groups follow the general structural and dynamical properties of the membrane, which renders them rather nonperturbing. Nevertheless, as all lipid segments, these probes are distributed broadly with regard to the bilayer normal, which suggests that distance measurements involving these probes should be analyzed with great caution. Finally, by carrying out a simple headgroup exchange also unsaturated analogs of other phospholipids, e.g., phosphatidylserine or phosphatidylethanolamine could be synthesized for membrane studies.

SUPPORTING MATERIAL

Synthesis of 1-palmitoyl-2-oleoyl-(16-doxyl)-*sn*-glycero-phosphocholine is available at http://www.biophysj.org/biophysj/supplemental/S0006-3495(08)00109-4.

We thank Sabine Schiller (Humboldt University Berlin) for technical assistance, Christoph Thiele (MPI Dresden) for helpful comments to chemical synthesis, and Michael von Löwis (Humboldt University Berlin) for carrying out MS analysis.

This work was supported by the Deutsche Forschungsgemeinschaft (PO 748/3, HU 720/5-2, and MU 1017/5).

REFERENCES

1. Binder, H. 2003. The molecular architecture of lipid membranes—new insights from hydration-tuning infrared linear dichroism spectroscopy. *Appl. Spectrosc. Rev.* 38:15–69.
2. Seelig, J. 1978. 31P nuclear magnetic resonance and the headgroup structure of phospholipids in membranes. *Biochim. Biophys. Acta.* 515:105–140.
3. Seelig, J., and A. Seelig. 1980. Lipid conformation in model membranes and biological membranes. *Q. Rev. Biophys.* 13:19–61.
4. Scheidt, H. A., and D. Huster. 2008. The interaction of small molecules with phospholipid membranes studied by 1H NOESY NMR under magic-angle spinning. *Acta Pharmacol. Sin.* 29:35–49.
5. Nagle, J. F., and S. Tristram-Nagle. 2000. Structure of lipid bilayers. *Biochim. Biophys. Acta.* 1469:159–195.
6. Marsh, D., D. Kurad, and V. A. Livshits. 2005. High-field spin-label EPR of lipid membranes. *Magn. Reson. Chem.* 43:S20–S25.
7. Bartucci, R., D. A. Erilov, R. Guzzi, L. Sportelli, S. A. Dzuba, et al. 2006. Time-resolved electron spin resonance studies of spin-labeled lipids in membranes. *Chem. Phys. Lipids.* 141:142–157.
8. Devaux, P. F., P. Fellmann, and P. Hervé. 2002. Investigation on lipid asymmetry using lipid probes: Comparison between spin-labeled lipids and fluorescent lipids. *Chem. Phys. Lipids.* 116:115–134.
9. Marsh, D. 1990. Lipid-protein interactions in membranes. *FEBS Lett.* 268:371–375.
10. Marsh, D. 2001. Application of electron spin resonance for investigating peptide-lipid interactions, and correlation with thermodynamics. *Biochem. Soc. Trans.* 29:582–589.
11. Marsh, D., and L. I. Horvath. 1998. Structure, dynamics and composition of the lipid-protein interface. Perspectives from spin-labeling. *Biochim. Biophys. Acta.* 1376:267–296.
12. Esmann, M., and D. Marsh. 2006. Lipid-protein interactions with the Na,K-ATPase. *Chem. Phys. Lipids.* 141:94–104.
13. Voelker, D. R. 1991. Organelle biogenesis and intracellular lipid transport in eukaryotes. *Microbiol. Mol. Biol. Rev.* 55:543–560.
14. Olayioye, M. A., S. Vehring, P. Müller, A. Herrmann, J. Schiller, et al. 2005. StarD10, a START domain protein overexpressed in breast cancer, functions as a phospholipid transfer protein. *J. Biol. Chem.* 280:27436–27442.
15. Bettebobillo, P., and M. Vidal. 1995. Characterization of phospholipase A(2) activity in reticulocyte endocytic vesicles. *Eur. J. Biochem.* 228:199–205.
16. Müller, K., T. Pomorski, P. Müller, and A. Herrmann. 1997. The use of spin-labeled phospholipid analogues to characterize the transverse distribution of phospholipids and the activity of phospholipase-A2 in the cell membrane of bull spermatozoa. *Adv. Exp. Med. Biol.* 424:243–244.
17. Rufini, S., J. Z. Pedersen, A. Desideri, and P. Luly. 1990. Beta-bungarotoxin-mediated liposome fusion: spectroscopic characterization by fluorescence and ESR. *Biochemistry.* 29:9644–9651.
18. Schewe, M., P. Müller, T. Korte, and A. Herrmann. 1992. The role of phospholipid asymmetry in calcium-phosphate-induced fusion of human erythrocytes. *J. Biol. Chem.* 267:5910–5915.
19. Chiang, Y. -W., J. Zhao, J. Wu, Y. Shimoyama, J. H. Freed, et al. 2005. New method for determining tie-lines in coexisting membrane phases using spin-label ESR. *Biochim. Biophys. Acta.* 1668:99–105.
20. Swamy, M. J., L. Ciani, M. Ge, A. K. Smith, D. Holowka, et al. 2006. Coexisting domains in the plasma membranes of live cells characterized by spin-label ESR spectroscopy. *Biophys. J.* 90:4452–4465.
21. Piknova, B., D. Marsh, and T. E. Thompson. 1997. Fluorescence quenching and electron spin resonance study of percolation in a two-phase lipid bilayer containing bacteriorhodopsin. *Biophys. J.* 72:2660–2668.
22. Vogel, A., H. A. Scheidt, and D. Huster. 2003. The distribution of lipid attached spin probes in bilayers: application to membrane protein topology. *Biophys. J.* 85:1691–1701.
23. Raja, M. M., and R. K. H. Kinne. 2005. Interaction of C-terminal loop 13 of sodium-glucose cotransporter SGLT1 with lipid bilayers. *Biochemistry.* 44:9123–9129.
24. Scheidt, H. A., P. Müller, A. Herrmann, and D. Huster. 2003. The potential of fluorescent and spin-labeled steroid analogs to mimic natural cholesterol. *J. Biol. Chem.* 278:45563–45569.
25. Marsh, D. 1981. Electron spin resonance: spin labels. *In* Membrane Spectroscopy. Molecular Biology, Biochemistry and Biophysics. E. Grell, editor. Springer-Verlag, Berlin, Heidelberg, New York. 51–142.
26. Schorn, K., and D. Marsh. 1996. Lipid chain dynamics and molecular location of diacylglycerol in hydrated binary mixtures with phosphatidylcholine: spin label ESR studies. *Biochemistry.* 35:3831–3836.
27. White, S. H., A. S. Ladokhin, S. Jayasinghe, and K. Hristova. 2001. How membranes shape protein structure. *J. Biol. Chem.* 276:32395–32398.
28. Gawrisch, K., N. V. Eldho, and I. V. Polozov. 2002. Novel NMR tools to study structure and dynamics of biomembranes. *Chem. Phys. Lipids.* 116:135–151.
29. Soubias, O., and K. Gawrisch. 2005. Probing specific lipid-protein interaction by saturation transfer difference NMR spectroscopy. *J. Am. Chem. Soc.* 127:13110–13111.
30. Morse, P. D. 1977. Use of the spin label tempamine for measuring the internal viscosity of red blood cells. *Biochem. Biophys. Res. Commun.* 77:1486–1491.
31. Keith, A., G. Bulfield, and W. Snipes. 1970. Spin-labeled neurospora mitochondria. *Biophys. J.* 10:618–629.
32. Davis, J. H., K. R. Jeffrey, M. Bloom, M. I. Valic, and T. P. Higgs. 1976. Quadrupolar echo deuteron magnetic resonance spectroscopy in ordered hydrocarbon chains. *Chem. Phys. Lett.* 42:390–394.
33. Sternin, E., M. Bloom, and A. L. Mackay. 1983. De-pake-ing of NMR spectra. *J. Magn. Reson.* 55:274–282.
34. Lafleur, M., B. Fine, E. Sternin, P. R. Cullis, and M. Bloom. 1989. Smoothed orientational order profile of lipid bilayers by 2H-nuclear magnetic resonance. *Biophys. J.* 56:1037–1041.
35. Huster, D., K. Arnold, and K. Gawrisch. 1998. Influence of docosahexaenoic acid and cholesterol on lateral lipid organization in phospholipid mixtures. *Biochemistry.* 37:17299–17308.
36. Bunge, A., P. Müller, M. Stöckl, A. Herrmann, and D. Huster. 2008. Characterization of the ternary mixture of sphingomyelin, POPC, and cholesterol: support for an inhomogeneous lipid distribution at high temperatures. *Biophys. J.* 94:2680–2690.
37. Kornberg, R. D., and H. M. McConnell. 1971. Inside-outside transitions of phospholipids in vesicle membranes. *Biochemistry.* 10:1111–1120.
38. Chattopadhyay, A., and E. London. 1987. Parallax method for direct measurement of membrane penetration depth utilizing fluorescence quenching by spin-labeled phospholipids. *Biochemistry.* 26:39–45.
39. Huster, D., P. Müller, K. Arnold, and A. Herrmann. 2001. Dynamics of membrane penetration of the fluorescent 7-nitrobenz-2-oxa-1,3-diazol-4-yl (NBD) group attached to an acyl chain of phosphatidylcholine. *Biophys. J.* 80:822–831.
40. Huster, D., and K. Gawrisch. 1999. NOESY NMR cross peaks between lipid headgroups and hydrocarbon chains: spin diffusion or molecular disorder? *J. Am. Chem. Soc.* 121:1992–1993.